Molecular Biology, Vol. 36, No. 5, 2002, pp. 736–753. Translated from Molekulyarnaya Biologiya, Vol. 36, No. 5, 2002, pp. 912–930.

STRUCTURAL–FUNCTIONAL ANALYSIS OF BIOPOLYMERS AND THEIR COMPLEXES

UDC 577.323

Interaction of Topotecan, DNA Topoisomerase I Inhibitor, with Double-stranded Polydeoxyribonucleotides. 4. Topotecan Binds Preferably to the GC Base Pairs of DNA

S. A. Strel'tsov[1], A. L. Mikheikin[1], S. L. Grokhovsky[1,2], V. A. Oleinikov[3], I. A. Kudelina[3], and A. L. Zhuze[1]

[1] *Engelhardt Institute of Molecular Biology, Russian Academy of Sciences, Moscow, 119991 Russia; E-mail: strelcov@imb.ac.ru*

[2] *University of Oslo Medical Research Center, Moscow, 119991 Russia*

[3] *Shemyakin and Ovchinnikov Institute of Bioorganic Chemistry, Russian Academy of Sciences, Moscow, 117871 Russia*

Received December 25, 2001

Abstract—Interaction of topotecan (TPT) with synthetic double-stranded polydeoxyribonucleotides has been studied in solutions of low ionic strength at pH 6.8 by linear flow dichroism (LD), circular dichroism (CD), UV-Vis absorption, and Raman spectroscopy. The complexes of TPT with poly(dG-dC)·poly(dG-dC), poly(dG)·poly(dC), poly(dA-dC)·poly(dG-dT), and poly(dA)·poly(dT), as well as complexes of TPT with calf thymus DNA and coliphage T4 DNA studied by us previously, have been shown to have negative LD in the long-wavelength absorption band of TPT, whereas the complex of TPT with poly(dA-dT)·poly(dA-dT) has positive LD in this absorption band of TPT. Thus, there are two different types of TPT complex with the polymers. TPT has been established to bind preferably to GC base pairs because its affinity to the polymers of different composition decreases in the following order: poly(dG-dC)·poly(dG-dC) > poly(dG)·poly(dC) > poly(dA-dC)·poly(dG-dT) > poly(dA)·poly(dT). The presence of DNA has been shown to shift the monomer–dimer equilibrium in TPT solutions toward dimer formation. Several duplexes of the synthetic polynucleotides bound together by bridges of TPT dimers may participate in the formation of the studied type of TPT–polynucleotide complex. Molecular models of TPT complex with linear and circular supercoiled DNAs and with deoxyguanosine have been considered. TPT (and presumably the whole camptothecin family) proved to represent a new class of DNA-specific ligands whose biological action is associated with formation of dimeric bridges between two DNA duplexes.

Key words: camptothecin, topotecan, linear flow dichroism, DNA binding, GC specificity

INTRODUCTION

This study is a continuation of a series of papers dealing with the interaction of topotecan (water-soluble derivative of camptothecin, human DNA topoisomerase I inhibitor) with double-helical nucleic acids in solutions of low ionic strength [1]. Alkaloid camptothecin (CPT) (Fig. 1) from *Camptotheca acuminata* was isolated in 1966 [2]. CPT and its synthetic derivatives were found to be human DNA topoisomerase I (topo I) inhibitors [3, 4]. Topotecan (TPT) (Fig. 1), a CPT analog showing substantially higher water solubility as compared with CPT, was synthesized in 1991 [3]. TPT shows anticancer activity and low toxicity, in contrast to CPT, which made possible its use in clinic [5]. The molecules of CPT family bind to DNA and topo I to give a triple complex and prevent religation of the sugar-phosphate backbone previously cleaved by this enzyme [6, 7]. It was supposed for a long time that CPT weakly interacts with DNA, especially with its linear form, and does not interact with topo I [6, 8, 9]. It has been shown recently that TPT binds to the DNA minor groove in solution of low ionic strength (1 mM sodium cacodylate) and pH 6.8 [1], and the DNA–TPT complexes can interact with each other [10]. The resulting struc-

0026-8933/02/3605-0736$27.00

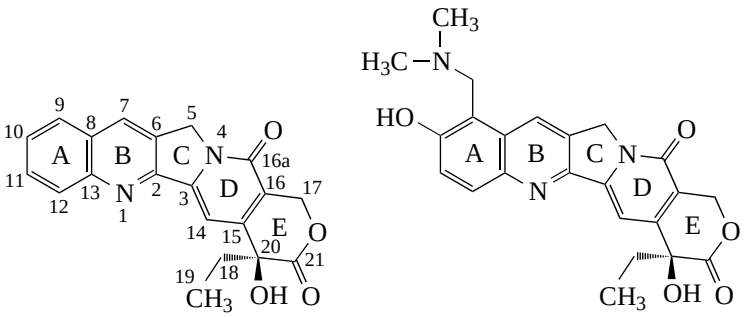

Fig. 1. Chemical structure of camptothecin and topotecan.

tures have negative LD in the long-wavelength absorption band of TPT [10]. There are two schools of thought as regards the binding specificity of TPT. Basing on indirect data, certain researchers believe TPT better binds to GC pairs of DNA [7, 11–15], while others prefer AT pairs, in particular thymine [16] or adenine [17]. The aim of this study was to reveal the binding specificity of TPT toward double-stranded DNAs. At low ionic strength, TPT showed the highest affinity to guanine, interacting with polymers preferably as dimers. We suppose polydeoxyribonucleotides to be capable of interacting with each other in the presence of TPT to yield complexes containing two or more polymer molecules. Models of TPT interaction with linear and circular supercoiled DNA and with deoxyguanosine are suggested.

EXPERIMENTAL

Materials. Topotecan from SmithKline Beecham was kindly provided by Prof. I.R. Nabiev, for physicochemical studies it was additionally purified and checked for homogeneity as described in [18]. We used sodium cacodylate and poly(dG)·poly(dC) from Sigma, poly(dG-dC)·poly(dG-dC), poly(dA-dT)·poly(dA-dT), poly(dA)·poly(dT) from P.-L. Biochemicals, poly(dA-dC)·poly(dT-dG) from Amersham Pharmacia Biotech.

Synthetic polymers were dissolved in 1 mM sodium cacodylate (pH 6.8) followed by dialysis at 4°C against the same buffer with its triple replacement. The duration of dialysis stage was at least 8 h, the ratio of DNA/buffer solution volumes in the dialysis was 1:15. The concentrations of poly(dG-dC)·poly(dG-dC), poly(dG)·poly(dC), poly(dA-dC)·poly(dG-dT), poly(dA)·poly(dT), and poly(dA-dT)·poly(dA-dT) were determined spectrophotometrically using the following molar extinction coefficients: ε_{254} = 16,800, ε_{253} = 14,800, ε_{260} = 13,200, ε_{262} = 12,000, ε_{260} = 13,200 $M^{-1}\,cm^{-1}$ per bp [19].The concentrations of polymers are given in moles (bp) per liter. Complexes of TPT with the polymers were obtained from concentrated solutions of polymers (~10^{-3} M) and TPT (~10^{-4} M). The measurements were performed in three days after complex preparation (in view of the low rate of complex formation [18]).

Spectral measurements. Optical density of solutions was measured on a Cary 118 spectrophotometer. CD spectra were recorded on a Jobin-Yvon Mark III dichrograph. LD was determined using the specially designed add-on unit to this dichrograph [20]. Details of LD determination see in [1]. Raman spectra were recorded with Ramanor HG-2S spectrometer. Excitation was accomplished using Spectra Physics 164-03 Kr^+ laser operating at λ = 647.1 nm. During Raman spectra recording, sample irradiation power was not higher than 200 mW. The spectra were recorded with the step of 2 cm^{-1} and integration time 3 s. Data treatment was performed with the use of LabCalc software package (Galactic Industries).

Quantum chemical calculations of CPT molecule. The long-wavelength electron transition dipole moment (ETDM) of camptothecin molecule was calculated as in [18].

RESULTS AND DISCUSSION

Estimated Structure of TPT Dimers in Solution

In the study on the TPT dimerization in solution, we suggested several types of structures (**I**, **II**) of its dimers [18]. They are shown in Figs. 2a and 2b. We have also shown that the hydroxy group of the A ring of TPT participates in dimer formation. However, this hydroxy group could form a hydrogen bond not only with the N1 atom as in suggested models, but also with the keto group of ring D. The structure of TPT dimers of this type (**III**) is shown in Fig. 2c. Three rings (A–C) overlap in this structure, whereas only one ring A overlaps in the dimers of the **I** and **II** types. The extent of monomer overlap in the TPT dimer of the **III** type is close to that in CPT dimer (data of

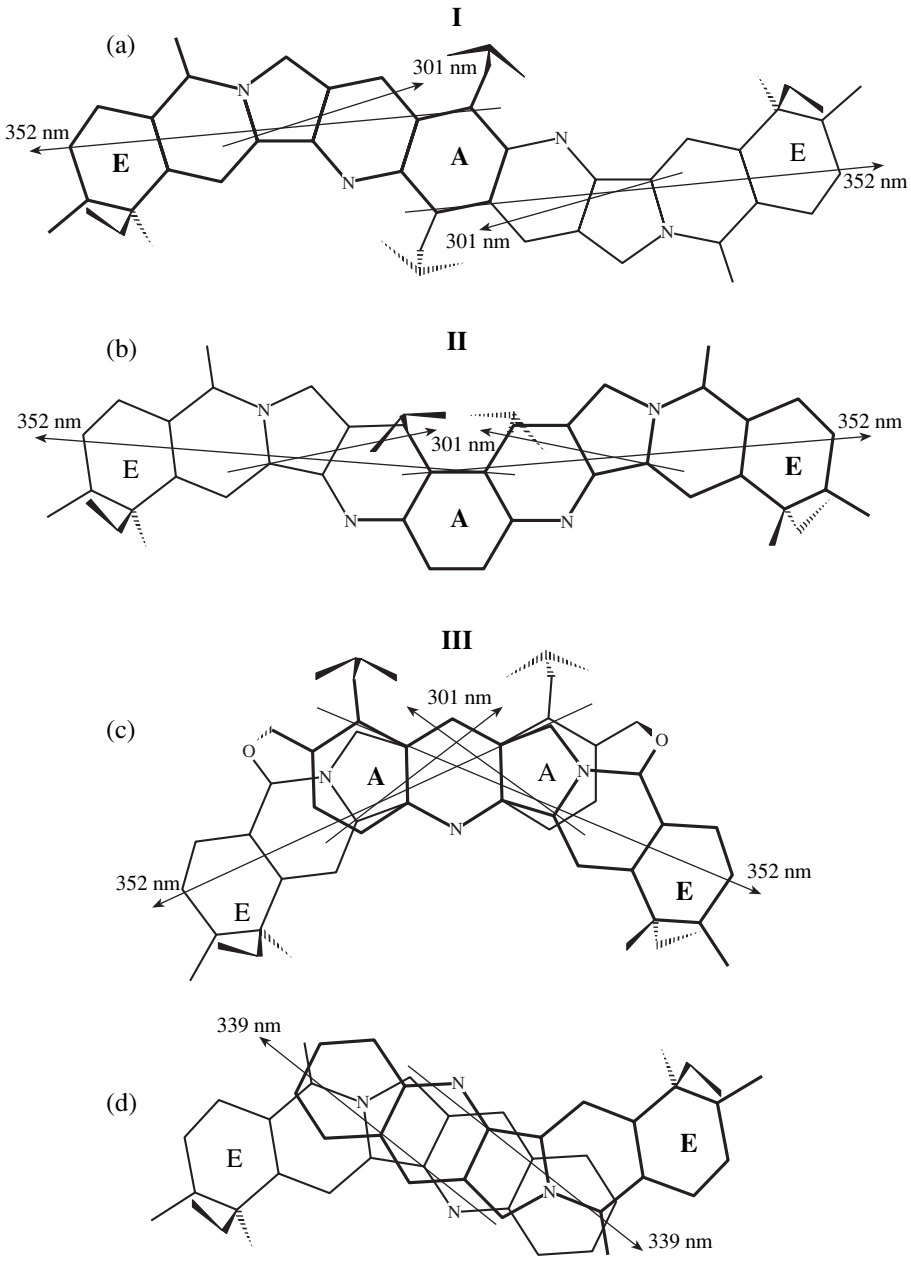

Fig. 2. Structure of TPT dimers of the **I** (a), **II** (b), and **III** (c) types and (d) CPT dimer. Arrows show the directions of long-wavelength ETDMs in ligand monomers, neighboring digits show the wavelength of corresponding transition. Thick lines show the upper monomer.

X-ray diffraction study [21]). Moreover, the keto group of the ring D having protonation pKa ~3.5 is more preferable as proton acceptor upon hydrogen bonding than N1 atom whose protonation pKa is only ~0.5. TPT dimers of the **III** type as those of the **II** type [18] could exist in two forms differing only by the orientation of the rings E of TPT monomers, which directed either out or into the dimer.

TPT dimers of the **I** type have a helical twofold symmetry axis perpendicular to the plane of rings A passing through their center and a pseudo-twofold symmetry axis going equidistant between the planes of the rings A of TPT monomers in the plane passing through the middles of bonds C8–C9 and C11–C12. The same axis is the twofold symmetry axis for the TPT dimer of the **II** type. The TPT dimer of the **III** type has twofold symmetry axis passing between and parallel to the planes of the rings B of TPT monomers in the plane of lines connecting atoms N1 and C7 in each monomer. Note that CPT dimer has a twofold symmetry axis perpendicular to the planes of the monomers and a pseudo-twofold symmetry axis pass-

ing equidistant between the planes of CPT monomers, i.e., CPT dimer is similar to the TPT dimer of the **I** type from symmetry viewpoint.

Our study of Raman spectra of TPT in solution has shown that the band in the region of 1300 cm^{-1} related to the deformation vibrations of hydroxy group of the ring A shifts from 1303 to 1307 cm^{-1} when TPT concentration in solution changes from 10^{-4} to 10^{-3} M. High-frequency band shift responsible for the deformation vibrations of hydroxy group is known to indicate the participation of this group in hydrogen bonding [22]. Thus, these results provide additional confirmation of previous data on the participation of this group in hydrogen bonding in TPT dimer [10]. It was also found that the band at 1653 cm^{-1} related to keto group vibrations did not change position and intensity [23, 24] upon the same variation in TPT concentration, although this band altered on the interaction of TPT with DNA [1]. Hence, one may conclude that the TPT dimer of the **III** type does not appear in solution in the form shown in Fig. 2c. This is strange, because the formation constant for the TPT dimer of this type should be much higher than for the TPT dimer of the **I** or **II** types, owing to substantially better stacking of the monomers to each other and stronger hydrogen bonding (the charge is –0.07 on the N1 atom but –0.34[1] on the oxygen atom at C16a). One may suppose that TPT dimer of the **III** type does not appear in solution because competition arises between hydrogen bonding and optimal stacking interaction where stacking interaction prevails.

Thus, among the TPT dimers stabilized by hydrogen bonding with the hydroxy groups of the rings A, only TPT dimers of the **I** and **II** types could occur in solution.

We have studied apparent molar dichroism spectra ($\Delta\varepsilon_{app} = \Delta D/C$) of free TPT to reveal the types of TPT dimers really occurring in solution. Figure 3c, curves 1 and 2, shows the spectra for TPT concentrations of $8.84 \cdot 10^{-6}$ and $1.99 \cdot 10^{-4}$ M, respectively. According to our data, TPT dimers are virtually absent in more dilute solution, while their content is ~50% in more concentrated solution [18]. For comparison, Fig. 3a shows the spectra of apparent extinction ($\varepsilon_{app} = A/C$) of TPT at concentrations $2.14 \cdot 10^{-5}$ and $2.14 \cdot 10^{-4}$ M, curves *1* and *2*, respectively. There are two types of CD spectra: conservative—"butterfly" type, which intersect zero line (have zero dichroism) at wavelength corresponding to maximum in absorption spectrum—and nonconservative, induced, which are similar to the absorption spectrum for given electron transition. Conservative CD spectra appear due to dipole–dipole interaction of molecules with the same chromophores, in particular upon dimerization. Nonconservative CD spectrum results from the influence of asymmetric environment on the studied chromophore. It follows from the shown CD spectra that TPT monomers have only nonconservative CD spectrum of positive sign at wavelength < 300 nm. It is induced by the presence of the chiral ring E in TPT molecule. The absence of induced CD spectrum of TPT monomers (see Fig. 3b, curve *1*) in the long-wavelength absorption region (~335–380 nm) indicates that the ring E has rather weak effect on the long-wavelength transitions in the molecule.

A CD spectrum appears for TPT molecules in the region of long-wavelength transitions when concentration rises (see Fig. 3b, curve *2*). This is the CD spectrum of TPT dimers because the monomers have no CD at these wavelengths. Absorption maxima at 380 and 335 nm correspond to inflection points or the points of intersection of CD spectrum with zero line, which is the feature of conservative CD spectrum. It should be noted that the bands at 380 and 335 nm split into two bands because of interaction with the solvent. The shoulder at 370 nm in the absorption spectrum corresponds to the inflection point in CD spectrum (see curves *2* in Figs. 3a and 3b). The fact that this inflection point is not the intersection point of CD spectrum with zero line is associated, in our opinion, with the superposition of the nonconservative CD spectrum on the conservative CD spectrum (in the region 380–335 nm). Its appearance may be due to the influence of the chiral ring E of one TPT monomer in dimer on the long-wavelength transitions of another monomer, which induces positive CD as in the case of short-wavelength CD spectrum of the monomers. Since the distance and orientation of the rings A and B in one TPT molecule and the ring E in another TPT molecule in the TPT dimers of the **I** and **II** types are almost the same as in TPT monomers, whereas the monomers have no CD spectrum in this region, then nonconservative CD spectrum will be absent for these types of TPT dimers. The appearance of nonconservative component in the CD spectrum of TPT dimers may indicate the presence of TPT dimers of the **IV** type in solution in which the overlap of TPT chromophores is substantially larger than in the TPT dimers of the **I** and **II** types. Indeed, induced CD arises when the rings A and B of one TPT monomer prove to be in close proximity to the ring E of another monomer and oriented in more favorable manner. Determination of the structure of TPT dimers of this type by optimization of dimer structure with HyperChem 4.5 software (HyperCube Inc., freeware version) using AMBER parametrization, on the one hand, led to a large overlap of the rings A–E of TPT monomers (structure not given), on the other hand, the chromophore overlap proved to be substantially larger than even in CPT dimer whose structure is shown in Fig. 2d (X-ray crystallography data [21]). Therefore such an optimized structure of TPT dimer could not be used in our studies even as a first approximation. It is

[1] The charges are given in electron charges.

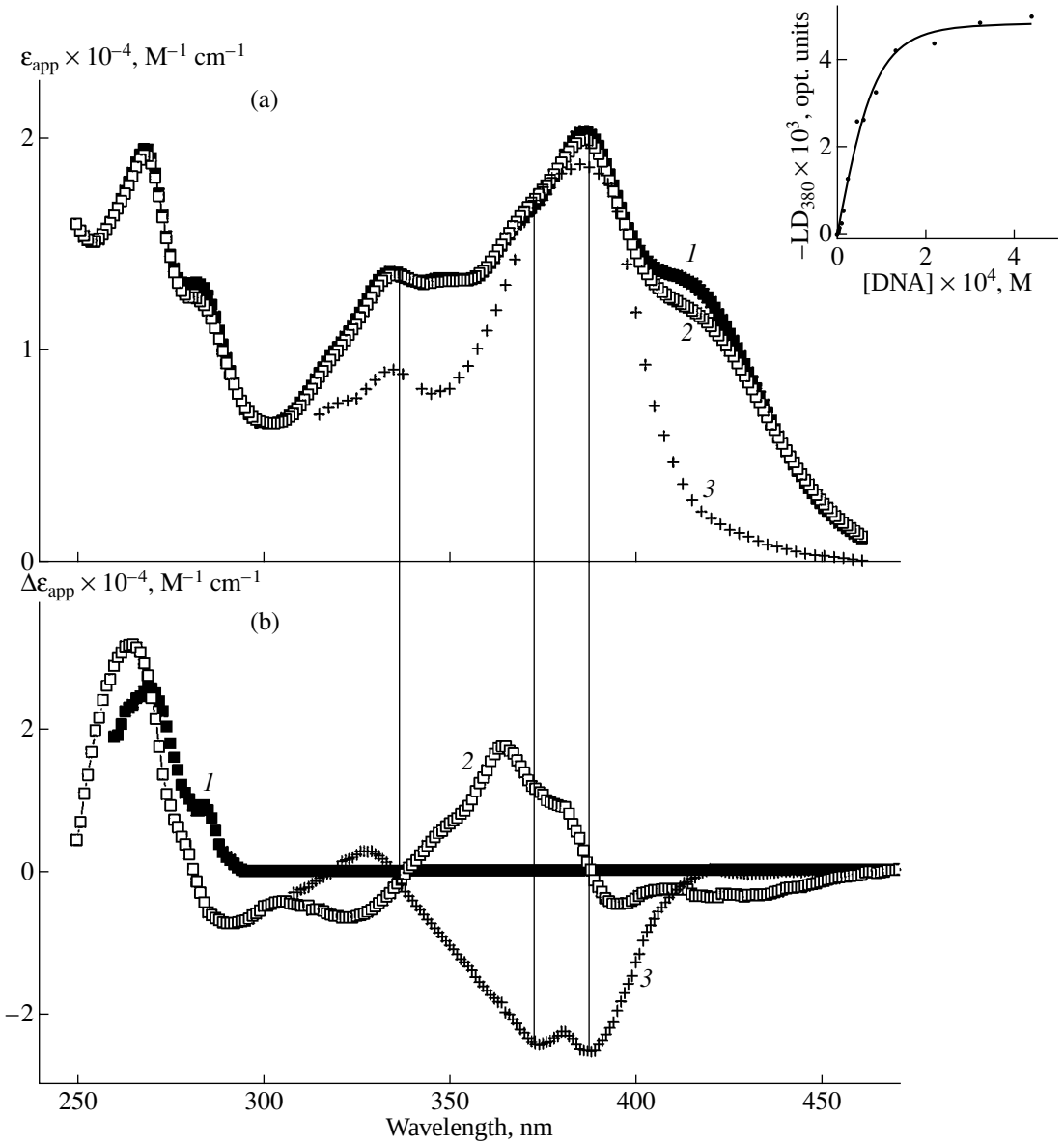

Fig. 3. Spectra of apparent extinction ε_{app} (a) and apparent molar dichroism $\Delta\varepsilon_{app}$ (b) for different TPT concentrations in a free state and in the presence of saturating DNA concentration; (a) ε_{app} spectra for $2.14 \cdot 10^{-5}$ M (*1*) and $2.14 \cdot 10^{-4}$ M TPT (*2*) and for complex of $1.35 \cdot 10^{-5}$ M TPT with $3.22 \cdot 10^{-4}$ M bp DNA (*3*). (b) $\Delta\varepsilon_{app}$ spectra for $8.84 \cdot 10^{-6}$ M (*1*) and $1.99 \cdot 10^{-4}$ M TPT (*2*) and complex of $9.95 \cdot 10^{-6}$ M TPT with $3.52 \cdot 10^{-4}$ M bp DNA (*3*). The dependence of linear dichroism LD_{380} of TPT ($1.35 \cdot 10^{-5}$ M) on DNA concentration is shown in the upper right-hand corner. Buffer: 1 mM sodium cacodylate, pH 6.8.

necessary to get more complete experimental data on this structure.

Thus, the emergence of nonconservative component of CD spectra for TPT dimer solutions indicates the existence of TPT dimers of the **IV** type with considerably larger chromophore overlap than in the TPT dimers of the **I** and **II** types.

Let us consider the conservative portion of CD spectrum of TPT dimers. The amplitude of this CD spectrum depends on the mutual orientation of the electron transition dipole moments (ETDMs) of the monomers in TPT dimer of one or another type. Figures 2a–2d show the orientation of long-wavelength ETDMs with respect to the structures of three types of TPT dimers and CPT dimer, respectively. We have calculated the orientations of ETDMs for TPT monomers earlier in [18] and for CPT in this work.

The rings E of both TPT monomers in the TPT dimer of the **I** type are disposed out of the plane of other rings and directed **"away from us"**. The projections of monomer long-wavelength ETDMs at 352 nm

on the plane of rings A–D are parallel each other for TPT dimers of the **I** type (see Fig. 2a), however they are tilted 9° **"toward us"**. In the dimer, the angle between them is 18° (supplementary). ETDMs at 301 nm are collinear because they lie in the plane of rings A–D (see Fig. 2a). Thus, the conservative CD spectrum for the TPT dimers of the **I** type will be observed in the band at 380 nm and will not be observed in the band at ~335 nm (calculated ETDM values at 301 and 352 nm correspond to experimentally observed absorption bands at ~335 and 380 nm). Hence, the presence of only TPT dimers of the **I** type in solution is insufficient to explain the observed conservative CD spectrum.

In the TPT dimer of the **II** type, the E rings of either TPT molecule can deviate from the plane of the rings A–D to different sides. There are two kinds of the deviation of rings E in the TPT dimers of this type: **in** and **out** with respect to the plane of the rings A–D. The long-wavelength ETDMs at 352 nm emerge from the ring plane to one side. On the other hand, in this kind of TPT dimer, the projections of monomer ETDMs at 352 and 301 nm on the chromophore plane form angles (supplementary) 8° and 20°, respectively (see Fig. 2b). Thus, for the TPT dimer of the **II** type, taking into account the angle formed by ETDM at 352 nm with the plane of rings A–D, the amplitudes of the bands of conservative CD at 335 and 380 nm will be almost the same (the calculated values of ETDMs at 301 and 352 nm correspond to experimentally observed absorption bands at ~335 and 380 nm).

The orientation of the E rings in the TPT dimer of the **III** type is the same as in the TPT dimer of the **II** type. However, as it follows from Fig. 2c, the projections of ETDMs of its monomers (at 352 and 301 nm) on the plane of the rings A–D form supplementary angles 72° and 46°, respectively. Therefore, in the spectrum of conservative CD, the amplitude of band at 335 nm will be slightly larger than at 380 nm (the calculated values of ETDMs at 301 and 352 nm correspond to the experimentally observed absorption bands at ~335 and 380 nm), and both these amplitudes will be considerably larger than for TPT dimers of **I** and **II** types. Indeed, it is known from the CD theory [25] that the amplitude of butterfly-type spectrum is maximal if monomer ETDMs form angles 45° and 135° and equals to zero if the angles are 0° or 90°.

DNA bases are turned relative to each other through an angle of ~36° (almost the same angle as for the long-wavelength ETDMs of monomers in the TPT dimer of the **III** type). They have much lower extinction at the absorption maximum than TPT monomers (~7000 and 20,000 M^{-1} cm^{-1}, respectively), but the molar dichroism at 280 nm ($\Delta\varepsilon_{280}$) for DNA bases is ~2.5 M^{-1} cm^{-1} [26], whereas the amplitude of the conservative portion of CD ($\Delta\varepsilon_{280}$) for TPT bound to DNA is ~0.5 M^{-1} cm^{-1}. The comparison of molar dichroism of DNA bases and TPT indicates that there is no marked amount of TPT dimers of the **III** type in solution. This agrees well with the above data on the Raman spectra of TPT solutions.

Since these amplitudes of conservative CD for TPT dimers of the **II** type at 335 and 380 nm should be almost equal, while conservative CD for TPT dimers of the **I** type should be observed only at 380 nm, the experimentally observed conservative component of spectrum of TPT dimers could be explained by the superposition of CD contributions of TPT dimers of the **I** and **II** types with predominant contribution from TPT dimers of the **II** type. Taking into consideration the nonconservative component of CD spectrum, we can speak of the presence of type **IV** dimers in solution at $1.99 \cdot 10^{-4}$ M TPT.

In the CPT dimer, the E rings are oriented **away from us**. The long-wavelength ETDMs of CPT monomers are tilted 22° **toward us**, i.e., the angle between them is 44°. This may cause the strong CD signal of CPT solutions [27].

It seems as though only one type of dimer could exist in solution whose formation constant is maximal since less stable types of dimers would transform into it, but this contradicts the experiment. The existence of several types of dimer is likely to be due to the presence of several energy minima of different depth separated by potential barriers. The fact that TPT dimer of the **III** type does not exist seems to be associated with the fact that the change in the geometry of this type of dimer resulting in hydrogen bonding violation and consequent growth of dimer potential energy is **continuously** counterbalanced by its larger decrease due to enhanced stacking interaction.

The TPT dimerization constant in solution was determined in [10]. Experimentally determined constant is the sum of formation constants of separate dimer types since there are several types of TPT dimer in solution [28].

Interaction of TPT Dimers with DNA

To elucidate whether TPT dimers interact with DNA, let us consider the wavelength dependence of ε_{app} for free TPT concentrations of $2.14 \cdot 10^{-5}$ and $2.14 \cdot 10^{-4}$ M shown in Fig. 3a (curves *1* and *2*, respectively). Inset in Fig. 3a shows the binding curve for $9.95 \cdot 10^{-6}$ M TPT with DNA obtained by measuring LD at 380 nm. This curve reaches a saturation at DNA concentration ~$3 \cdot 10^{-4}$ M, it follows therefrom that all TPT molecules are bound to DNA at this and higher DNA concentrations. Therefore we prepared a complex containing $1.35 \cdot 10^{-5}$ M TPT and $3.22 \cdot 10^{-4}$ M DNA and recorded the spectrum of ε_{app}. It is shown in Fig. 3a, curve *3*. Increase in TPT concentration from

10^{-5} to 10^{-4} M results in decrease of shoulder at 420 nm. It has been shown earlier on spectra that decrease of the shoulder at 420 nm in TPT spectrum at constant pH is associated with formation of TPT dimers [18]. The binding of TPT to DNA leads to complete disappearance of this shoulder in TPT absorption spectrum. Consequently, the addition of DNA to TPT solution leads to increase in the concentration of TPT dimers in solution, which indicates the preferable interaction of TPT dimers with DNA. On the other hand, the addition of DNA to TPT solution under our ionic conditions was accompanied by quenching of TPT fluorescence (excitation at 390, registration at 530 nm) [10]. Although such quenching may result from several reasons, the presented data agree well with preferable binding of TPT dimers to DNA, since TPT dimers fluoresce less than the monomers [18]. The data on Raman spectra and surface-enhanced Raman scattering (SERS) of TPT solutions at different concentrations and TPT–DNA complexes also confirm the increase in TPT dimer concentration in the presence of DNA [23, 24, 29]. Thus, optical absorbance, fluorescence intensity, Raman spectra, and SERS indicate preferable binding of DNA to TPT dimers as compared with monomers.

To reveal the type of TPT dimers that binds preferably to DNA, we obtained $\Delta\varepsilon_{app}$ spectrum of complex of $9.95 \cdot 10^{-6}$ M TPT with $3.52 \cdot 10^{-4}$ M DNA, Fig. 3b, curve *3*. Instead of CD spectrum of positive sign typical for free TPT dimers, a CD spectrum of negative sign with almost the same shape appears, i.e., the CD spectrum of bound TPT dimers has mainly nonconservative character.

The negative sign of the nonconservative component of CD spectrum of bound TPT indicates that the long axis of TPT dimer of the **I** type (more exactly, ETDM corresponding to the observed transition at 380 nm) forms an angle with the plane of base pair (more precisely with the symmetry axis of base pair directed to the DNA minor groove) lesser 45°.

Since the contribution of conservative component to the CD spectrum of bound to DNA TPT dimers is low, the TPT dimers of the **I** type are the main representatives among bound to DNA TPT dimers because only they have weak conservative CD. Slight difference between absorption spectrum and CD spectrum for bound TPT molecules is observed only in the absorption band at 335 nm where CD spectrum undergoes a sort of inversion with respect to the CD spectrum of free monomers, while the point of intersection with zero line still almost coincides with the absorption maximum of bound to DNA TPT dimers (see Fig. 3a, curve *3*). This feature of CD spectrum in the region of 335 nm could be explained as a superposition of small conservative CD spectrum on the nonconservative component of CD spectrum. TPT dimers of the **II** type bound to DNA in small quantity may be responsible for this conservative spectrum (TPT dimer of the **I** type has no conservative component of CD spectrum in this band).

As we have shown above, TPT occurs in solution as dimers at least of three types, hydroxy group of ring A participating in the formation of only the **I** and **II** types. The presence of several types of TPT dimers in solution provides an explanation of apparent paradox observed in absorption spectra: conversion of about a half of monomers into dimers is accompanied by incommensurably small decrease in the shoulder at 420 nm, whereas binding to DNA leads to complete disappearance of this shoulder. This paradox could be solved assuming that not all dimers in solution are the dimers of **I** and **II** types whose formation results in complete disappearance of the shoulder at 420 nm in TPT absorption spectrum. Thus we obtain additional confirmation for the presence of TPT dimers of the **IV** type in solution. Complete binding of TPT to DNA, i.e., TPT binding with large excess of DNA, leads to the conversion of dimers of **all** types into a dimer that binds to DNA. This is similar to the transformation of the carboxy form of TPT into the lactone form in the presence of DNA excess in solution, since only the lactone form can bind to DNA [1]. Thus, the complete disappearance of the shoulder at 420 nm from the absorption spectrum of bound TPT indicates that TPT dimers of the **IV** type do not form the studied type of TPT–DNA complex (having negative LD at 380 nm), although they are present in solution in a considerable amount.

Thus, absorption, Raman, SERS, and CD spectra of TPT bound to DNA indicate that TPT dimers bind to DNA in solutions of low ionic strength with higher affinity than monomers, these dimers are likely to be type **I** dimers with a small contribution of type **II**.

TPT Binds Preferably to GC Pairs of DNA

To determine which DNA bases preferentially bind with TPT, a concentrated solution of one of the following polymers—poly(dG-dC)·poly(dG-dC), poly(dG)·poly(dC), poly(dA-dC)·poly(dG-dT), poly(dA)·poly(dT), and poly(dA-dT)·poly(dA-dT)—was added in portions to $9.8 \cdot 10^{-6}$ M TPT solution and LD_{380} was measured for each addition. TPT is known to have no LD in a free state. The appearance of LD in the ligand absorption band beyond polymer absorption band upon mixing of TPT and polymer solutions indicates that the ligand binds to the polymer. The addition of the polymers was continued until LD_{380} value became constant, indicating that all TPT molecules from solution have bound to the polymer. Figure 4a shows dependence of LD_{380} on the concentration of poly(dG-dC)·poly(dG-dC), poly(dG)·poly(dC), poly(dA-dC)·poly(dG-dT), poly(dA)·poly(dT), and

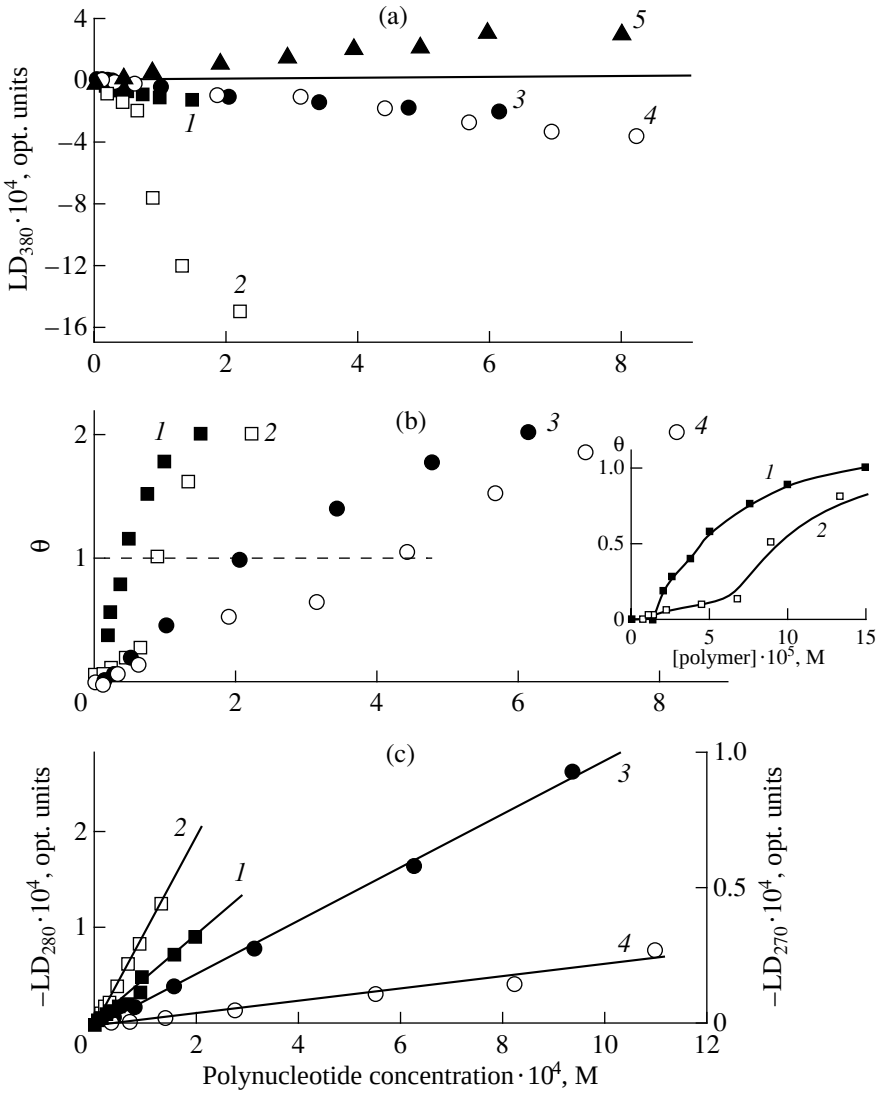

Fig. 4. Dependences of LD of free polydeoxyribonucleotides and their complexes with TPT on the concentrations of the polymers in solution. (a) Dependence of LD_{380} of TPT at $9.8 \cdot 10^{-6}$ M TPT on the concentration of poly(dG-dC)·poly(dG-dC) (*1*), poly(dG)·poly(dC) (*2*), poly(dA-dC)·poly(dG-dT) (*3*), poly(dA)·poly(dT) (*4*), and poly(dA-dT)·poly(dA-dT) (*5*) in solution. (b) Dependence of share θ of polymer-bound TPT molecules on the concentration of poly(dG-dC)·poly(dG-dC) (*1*), poly(dG)·poly(dC) (*2*), poly(dA-dC)·poly(dG-dT) (*3*), poly(dA)·poly(dT) (*4*) in solution. Inset: initial region of these dependences for poly(dG-dC)·poly(dG-dC) (*1*), poly(dG)·poly(dC) (*2*). (c) Right axis, dependence of LD_{270} for poly(dG-dC)·poly(dG-dC) (*1*); left axis, dependence of LD_{280} for poly(dG)·poly(dC) (*2*), poly(dA-dC)·poly(dG-dT) (*3*), poly(dA)·poly(dT) (*4*). *1*, black squares; *2*, empty squares; *3*, black circles; *4*, empty circles; *5*, black triangles. Buffer as in Fig. 3.

poly(dA-dT)·poly(dA-dT): curves *1*, *2*, *3*, *4*, and *5*, respectively.

It follows from these dependences that positive LD_{380} is observed when poly(dA-dT)·poly(dA-dT) is added to TPT, whereas the addition of any other polymer results in negative LD_{380}. Consequently, another type of complex results from TPT binding to poly(dA-dT)·poly(dA-dT), which should be studied elsewhere.

The curves of TPT binding to poly(dG-dC)·poly(dG-dC), poly(dG)·poly(dC), poly(dA-dC)·poly(dG-dT), poly(dA)·poly(dT) are S-shaped, which is most appreciable for the adsorption of TPT on homo- and hetero-GC polymers (see inset in Fig. 4b). The sign of LD effect and the shape of the binding curves are similar to those observed earlier for TPT complexes with calf thymus DNA and coliphage T4 DNA [1]. Therefore we consider TPT to form the same type of complex with DNA and these polymers. TPT concentration was the same in all experiments, but the saturation level of LD_{380} value was different for all the curves. This may be due to all the polymers

have different length. Indeed, LD_λ is determined by the formula [30]:

$$LD_\lambda = (A_\parallel - A_\perp)_\lambda = 3/2(3\cos^2\alpha - 1)A_\lambda S, \quad (1)$$

where α is the angle formed by ETDM of nucleic base or ligand with the DNA long axis which absorb light at wavelength λ; $A_\parallel$, $A_\perp$, and A_λ are the absorptions of light polarized parallel, perpendicular to flow and nonpolarized at wavelength λ, respectively; S is the factor of orientation ability of macromolecule in flow, which depends also on its length and rigidity.

To compare the curves of TPT binding to the polymers of different length, normalization was made: LD_{380} value corresponding to the i-th addition of polymer was divided by the maximal value $LD_{380,\,max}$ for this polymer, which corresponds to completely bound TPT, to give θ value, which equals to the portion of bound TPT. Figure 4b shows concentration dependence of θ for all studied polymers except for poly(dA-dT)·poly(dA-dT). As a control, Fig. 4c shows the concentration dependence of LD_{280} and LD_{270} in the polymer absorption region in the absence of TPT in solution. The dependences shown in Fig. 4c are linear. Consequently, the S-shaped curves in Fig. 4b, as in the case of TPT binding to DNA [11], are due to the interaction of TPT with the polymers rather than to changes in polymer structure upon an increase of their concentration.

It was shown previously that TPT can form with DNA several complexes containing different numbers of DNA duplexes [10] each of which has its own LD value per bound TPT molecule. Therefore, we used an approximate method to determine the affinity of TPT toward the polydeoxyribonucleotides. We determined polymer concentrations that bind half of the TPT molecules available in solution. Obviously, the lower polymer concentration is necessary for binding half of the TPT molecules the higher TPT affinity toward this polymer. Dotted line in Fig. 4b shows the level of 50% binding. According to this criterion, the affinity of TPT toward the polydeoxyribonucleotides decreases in the following order: poly(dG-dC)·poly(dG-dC) > poly(dG)·poly(dC) > poly(dA-dC)·poly(dG-dT) > poly(dA)·poly(dT). The binding specificity indicates that TPT affinity toward GC pairs is much higher than toward AT pairs.

Thereby, the assumed [16, 17] preferable binding of TPT to AT pairs (thymine or adenine) has not been confirmed experimentally. Indeed, this assumption was based on the fact that ^{1}H NMR spectra of TPT upon its interaction with thymine-containing polymers showed larger changes than upon its interaction with polymers containing guanine and no thymine [16]. The assumption on the preferable binding of CPT to adenine was based on the fact that the absorption spectrum upon mixing of CPT with different nucleosides changed only in the presence of adenosine [17]. However, the extent of the change is not in one-to-one correspondence with the affinity. Indeed, let us consider Fig. 4a: the amplitude of changes in LD_{380} upon TPT interaction with poly(dA)·poly(dT) is larger than with poly(dG-dC)·poly(dG-dC), whereas it is poly(dG-dC)·poly(dG-dC) that has higher affinity toward TPT (see Fig. 4b).

It has been shown recently that TPT localizes in the minor groove upon binding to DNA and poly(dG-dC)·poly(dG-dC) [1]. It is shown above that TPT binds preferably to GC base pairs. In the minor groove, AT and GC pairs differ only by the presence of the 2-amino group in guanine. Hence, TPT interacts with this group to form a hydrogen bond. This conclusion was confirmed in the direct study of TPT interaction with dG, dC, dA, dT, and dI with the use of Raman spectroscopy [31]. Only in the case of TPT–dG complexes, the Raman spectrum was the same as for the complexes with calf thymus DNA. On the other hand, our Raman spectral study of TPT–DNA complexes in solution showed no changes in the vibrations of the A and B rings except for those associated with an increase in the concentration of TPT dimers. This indicates that rings A and B do not participate in the interaction with DNA upon binding. Only keto groups of rings D and E could form hydrogen bonds with the 2-amino group of guanine. When the studied complex of TPT dimers with DNA arises (in solutions of low ionic strength), the long axis of the TPT molecule forms an angle of ~35° with the plane of bases [1, 10, 31]. The arrangement of these groups in TPT and the orientation of the TPT dimer with respect to DNA base pairs prevent for sterical reasons the simultaneous interaction of TPT with DNA via both keto groups. We have supposed [31] that the keto group of ring E is more preferable for binding to guanine, since the neighboring hydroxy group at C20 would form an additional hydrogen bond with N3 of the same guanine. It was established, however, that substitution of this hydroxy group with halogen atoms incapable of hydrogen bonding had little effect on the ability of such CPT derivatives to inhibit topo I [32]. Consequently, this hydroxy group does not take part in the hydrogen bonding of TPT with nucleic bases. Moreover, it was shown in [15] that a CPT derivative containing chloromethyl group at the 7th position is capable of covalent binding through this group to DNA base at position +1 from the topo I cleavage site, i.e., the supposed binding site of CPT and the binding site of TPT. The size of the chloromethyl group is so small that CPT and its derivatives (we assume a general mechanism of interaction with DNA for all CPT derivatives) can interact with DNA via groups in close proximity to the 7th position of CPT or TPT. Since C7 is substantially closer to C16a than to C21 (see Fig. 1), we should admit that our assumption [31] about TPT interaction with DNA via the keto group of ring E is

insufficiently grounded, and suppose the keto group of ring D to be more preferable as a proton acceptor in hydrogen bonding between TPT and the 2-amino group of guanine. Only further experimental studies can elucidate which keto group of TPT interacts with DNA.

Multiduplex Complexes of TPT with Polydeoxyribonucleotides

To explain the different affinity of TPT toward poly(dG)·poly(dC), poly(dG-dC)·poly(dG-dC), and poly(dA-dC)·poly(dG-dT), we have to consider the structure of TPT complex with double-helical polymers. It has been noted above that the S-shaped curves of TPT binding to most of the polymers studied in this work and the appearance of negative LD_{380} of bound TPT molecules indicates that the nascent complex is similar to the multiduplex complex of TPT with calf thymus DNA described earlier [10]. Polymer molecules (Fig. 4c) could not associate with each other within the studied concentration range in the absence of TPT. Of course, the fact that the polymers do not form quadruplet structures in the absence of TPT does not prove that it is TPT molecules that integrate DNA duplexes into a quadruplex. The effect of TPT on quadruplex formation can be indirect as, for example, in the case of interaction of trivaline with DNA; however, trivaline interacts with two neighboring DNA bases, which strongly alters the DNA structure [33, 34]. TPT appears to interact with only one base pair, moreover, with only one base so that the DNA structure is only weakly disturbed structure and is unable to interact with another such structure. It is most probable that it is TPT molecules that form "clips," "bridges" between two neighboring DNA duplexes. It is shown above that TPT dimers bind to DNA with a higher constant than monomers do. Thus, we suppose TPT dimers to be the "clips" that integrate DNA molecules into a multiduplex structure.

The following conditions must be fulfilled for TPT dimer to interact with two linear DNA molecules (Fig. 5):

(1) DNA duplexes should be parallel to each other;

(2) the monomers of the TPT dimer, to a first approximation, are to be located in the planes of the bases H-bonded with them in different DNA duplexes; as a result, the DNA duplexes prove to be shifted by one base with respect to each other along the axes (Z, Z_1);

(3) two duplexes, in terms of rotation about their long axes (Z and Z_1 in Fig. 5), should be mutually oriented in such a manner that the monomers of TPT dimer would form hydrogen bonds with the bases of its own duplex.

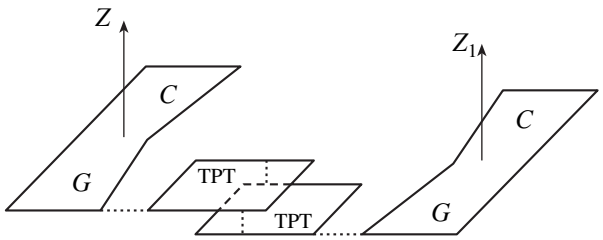

Fig. 5. Scheme of complexation of TPT dimer with two DNA duplexes. Parallelograms are TPT monomers. Irregular pentagons are GC pairs of DNA bases. Dotted lines show hydrogen bonds. Z and Z_1 are directions of long axes of DNA duplexes.

These conditions for the "synchronization" of DNA molecules with respect to each other upon formation of multiduplex structures are partly described in [35]. However, only one contact could form between neighboring DNA molecules under that conditions. For the formation of **regular** contacts, DNA molecules producing a quadruplex structure must have an integer period, i.e., an integer number of base pairs per turn. Only the fulfillment of these conditions could result in the formation of regular "clips" of TPT dimers between two DNA molecules. The binding constant of two DNA duplexes in the presence of saturating TPT concentrations is $\sim 10^4$ M^{-1} [10]. Of course, it is theoretically admissible that the "clips" arise after two, three, or more turns of DNA molecule rather than each turn, but the rarer these "clips" the lower the binding constant for the complex. Therefore, to a first approximation, let us suppose these "clips" to be disposed at each turn of the DNA molecule.

However, in terms of complexation of TPT dimers with only two polymer duplexes, it is difficult to explain the different TPT affinity toward poly(dG-dC)·poly(dG-dC), poly(dG)·poly(dC), and poly(dA-dC)·poly(dG-dT). Indeed, every tenth nucleotide pair in these polymers is GC and therefore the affinity of TPT toward all three sequences should have been the same. One of the possible reasons for the different affinity may be the structural difference of these polymers. The participation of more than two duplexes in the formation of TPT–DNA complex shown earlier [10] provides an alternative explanation.

To form a "flat" structure containing three or more DNA duplexes, the period of the polymers must be not only integer, but also even. Only then the DNA duplex will contain such a base pair that is turned through 180° with respect to the first one. Figure 6a is a schematic representation of such a structure. Moreover, hypothetically possible is the formation of the following TPT–DNA complexes containing three and more DNA duplexes but having another shape: (1) closed "tubular" structures produced by the first and *m*th bp

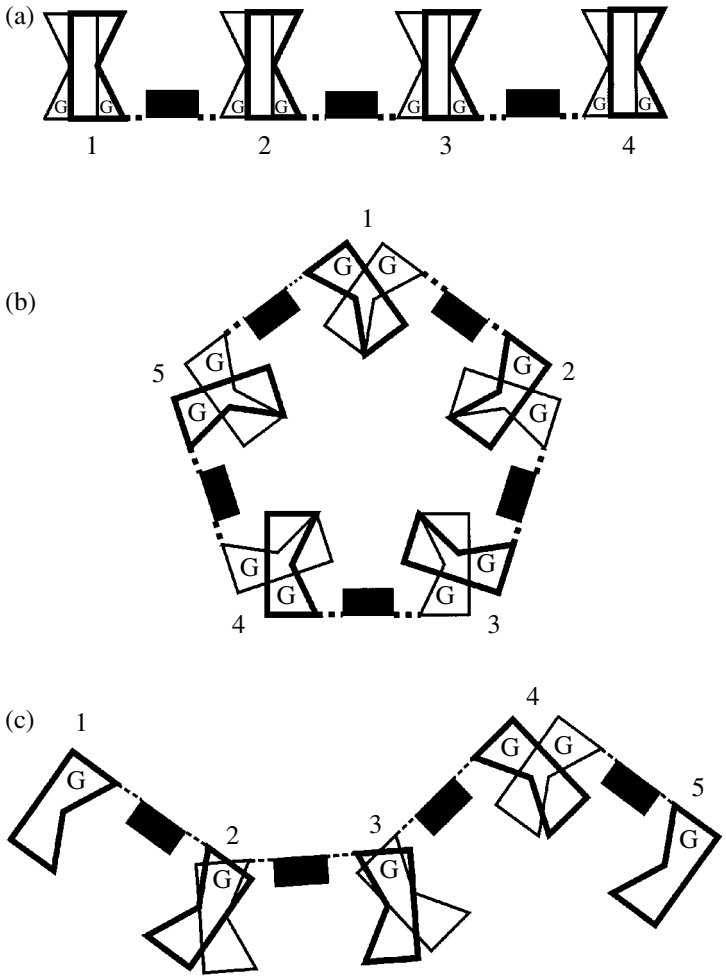

Fig. 6. Scheme of formation of TPT dimer–DNA multiduplex complexes. Digits indicate DNA duplexes: (a) flat, (b) tubular, (c) broken line. Black rectangle is TPT dimer. Pentagon is GC pair. Thick lines show GC pair located atop in the duplex. Dotted lines show hydrogen bonds. Letter G designates the position of guanine base in GC pair.

of each duplex, the *m*th bp being turned through the angle $\gamma_m = 36° \times m$ with respect to the first one (Fig. 6b exemplifies one such structure, a decaplex); (2) most general structures of "broken line" type where the first and arbitrary *i*th bp of each duplex participate in structure formation, which results in right-hand and left-hand bends in a random manner and by a random but discrete angle γ_i multiple of 36° (Fig. 6c). Considering these hypothetical structures, one should take into account the possibility of sterical hindrances due to interpenetration of atoms into each other. However, detailed examination of these structures is beyond the scope of the present work. Under our conditions, the resulting structures contain 3–4 DNA duplexes on average as shown in [10].

To analyze experimental results, it is sufficient that two DNA duplexes linked by "bridges" of TPT dimers can integrate a third duplex via the same "bridges." Then, upon formation of hexa- and more multiple structures of TPT complexes with polydeoxyribonucleotides, the TPT dimer will combine with the polymer every 5 rather than 10 bp. Therefore, if GC in poly(dG-dC)·poly(dG-dC), poly(dG)·poly(dC), poly(dA-dC)·poly(dG-dT) is considered as the first pair, then the sixth pair will be CG, GC, or TA, respectively. We have shown above that TPT binds to AT much weaker than to GC. Thus, poly(dA-dC)·poly(dG-dT) polymer in the presence of TPT will produce structures containing three or more duplexes with a lower constant than in the case of poly(dG-dC)·poly(dG-dC) and poly(dG)·poly(dC), since the third duplex will be linked to the quadruplex by interaction with AT, which is weaker than that with GC.

Some reproducible from experiment to experiment difference in the affinity of TPT toward poly(dG-dC)·poly(dG-dC) and poly(dG)·poly(dC), which have either CG or GC as every first and every sixth pair, remains unclear. This difference may be

explained by certain conformational changes of these polymers. But we suppose the reason to be the concatemerization of poly(dG-dC)·poly(dG-dC) in the presence of TPT. The ability of the polymers to form in the presence of TPT complexes containing several polydeoxyribonucleotide molecules provides a background for this process. To check this assumption, let us consider the data on $LD_{r,\lambda}$ for the free polymers and their complexes with TPT. The magnitude of $LD_{r,\lambda}$ is determined by the formula [30]:

$$LD_{r,\lambda} = 3/2(3\cos^2\alpha_\lambda - 1)S. \quad (2)$$

The designations are the same as in (1). It follows from formula (2) that $LD_{r,\lambda}$ depends on the angle α_λ formed by the ETDM of base or the ETDM of bound ligand with polymer long axis and on *S*, the factor of orientation ability of the macromolecule (in a free state or in the complex with ligand). The values of $LD_{r,280}$ and $LD_{r,380}$ were measured for poly(dG-dC)·poly(dG-dC), poly(dG)·poly(dC), poly(dA-dC)·poly(dG-dT), poly(dA)·poly(dT) in a free state and in the complex with TPT. The obtained values for free complexes are 0.010, 0.165, 0.022, and 0.056, respectively. For TPT–polymer complexes they are 0.0067, 0.0764, 0.0112, 0.0191. For the all four polymers, the value of $LD_{r,380}$ for TPT–polymer complex is lower than $LD_{r,280}$ for the free polymers. This is due to the measurements having been performed in the absorption band of TPT whose ETDM forms with the long axis of polymer an angle smaller than does ETDM of bases. On the other hand, there is no qualitatively significant change of $LD_{r,380}$ for the TPT–poly(dG)·poly(dC) complex as compared with other polymers. Thus, our assumption about concatenation of poly(dG)·poly(dC) molecules in the presence of TPT has not been confirmed experimentally.

However, the large value of $LD_{r,\lambda}$ for free poly(dG)·poly(dC) is conspicuous in comparison with other polymers, although the spread of values for these polymers is rather large. Since all bases form almost the same angle with the long axis of the polymers, the difference in the $LD_{r,\lambda}$ value between the polymers is associated with their orientation ability in a flow, i.e., their different length and/or rigidity. There was no concentration dependence of $LD_{r,280}$ value for poly(dG)·poly(dC), i.e., no formation of multiduplex structures by this polymer in the absence of TPT (see Fig. 4c). Thus, the cause of the larger $LD_{r,280}$ for free poly(dG)·poly(dC) remains unclear.

In the case of formation of multiduplex structures by DNA molecules in the presence of TPT, it is doubtful that $LD_{r,280}$ and $LD_{r,380}$ values can be used to determine the angle formed by the polymer long axis with ETDM of TPT at 380 nm as in [36], because it is not clear that the parameter *S* in formula (2) characterizing the rigidity of free polymers remains unchanged upon their complexation with TPT.

Molecular Model for the Interaction of TPT Dimers with Two Linear DNA Molecules

On the basis of data obtained both earlier [1, 10, 18] and in the present work, we have built a molecular model of complex of TPT dimer with DNA appearing in solutions of low ionic strength. The model has to satisfy the following restrictions: (1) TPT dimer interacts with two parallel DNA duplexes; (2) two hydrogen bonds arise between the keto groups of rings D of TPT dimer and the 2-amino groups of two guanines. Figures 7a and 7b show the model of complex of TPT dimer of the **I** type with two molecules of poly(dG)·poly(dC), view from the side of the long axis of poly(dG)·poly(dC) and view from the side of pseudo-twofold symmetry axis of TPT dimer, respectively. To avoid interpenetration of TPT atoms and polymer atoms in building this molecular model, we have to tilt TPT dimer by ~55° with respect to the DNA long axis, which agrees well with the LD data [1, 10]. In the model for the complex of TPT dimer of the **II** type with two DNA duplexes, the oxygens of phosphate groups of different DNA duplexes turn out to be at the distance down to 4.5 Å (note that this distance is at least 6 Å for the model of complex of TPT dimer of the **I** type). On the other hand, some oxygens of phosphate groups in quadruplex G4 are 3.5 Å apart [37]. Although the possibility to form multiduplex structure with the aid of TPT dimers of the **II** type remains questionable, in any case such a structure is less probable than that formed by the TPT dimers of the **I** type. We failed to build similar model using TPT dimers of the **III** type because of interpenetration of atoms of TPT and the polymer. This result is consistent with CD data indicating that TPT dimers of the **III** type do not participate in the formation of such a complex.

Molecular Model of Interaction of TPT Dimers with Circular Supercoiled DNA

We could not study this type of TPT–DNA complex by physicochemical methods for the reason below. The authors [17] have shown that the affinity of CPT (from which TPT is derived) toward circular supercoiled DNA is much higher than toward linear one, whereas the number of sites for CPT binding to the DNA almost equals the number of intramolecular contacts of duplex portions with each other (~1:500 bp). We supposed earlier [10, 31] that TPT dimers could form "bridges" between two duplexes or two parts of the same DNA duplex. Hence, the preferable binding sites of TPT dimers are to be the contact sites of two parts of the same duplex of circular supercoiled DNA. Note that these binding sites are also the sites of pref-

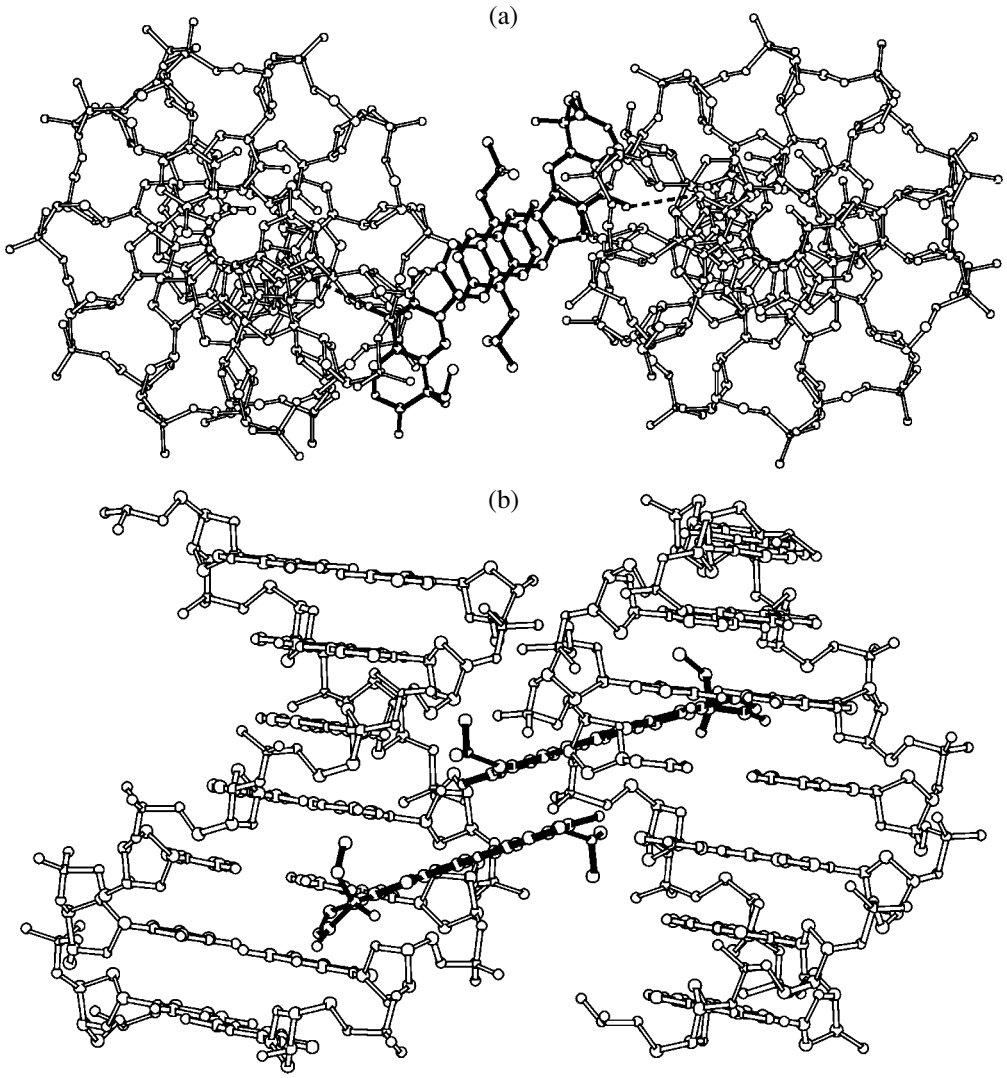

Fig. 7. Molecular model for the complex of TPT dimer (bold) of the **I** type with two parallel DNA duplexes. (a) View from the side of the DNA long axes. Dotted lines show hydrogen bonds between keto groups of rings D of TPT and 2-amino groups of guanines; (b) view from the side of the pseudo-twofold symmetry axis of TPT dimer located between and parallel to the planes of TPT monomers.

erable binding of topo I to DNA [38]. Because of the very low density of such sites on circular supercoiled DNA, the physicochemical study of these complexes of CPT (TPT) is extremely difficult. However, linear DNA acquires a rod-like structure in solutions of low ionic strength owing to considerable growth of its persistent length. This structure is the model for studying the sites of CPT (TPT) binding to circular supercoiled DNA since, in the context of above not stringent terms, the contact sites of two DNAs may repeat every 10 bp [10]. Increase in the solution ionic strength leads to decrease in the persistent length of DNA. The DNA becomes more flexible. Therefore it is impossible to form "bridges" from TPT dimers between DNA duplexes over any extended region and therefore intermolecular complex of TPT dimers with linear DNA molecules decomposes [10]. On the other hand, the increase in the solution ionic strength even leads to the growth in the number of contacts of duplex regions of circular supercoiled DNA with each other, i.e., the complexes of TPT dimers with such a DNA will exist also at physiological ionic strength of solution.

Figure 8 shows a molecular model for the complex of TPT dimer of the **I** type with the contact site of two duplexes. Figure 8a is a view from the side of the helical twofold symmetry axis of TPT dimer, which is perpendicular to its plane. Figure 8b is a view from the side of the pseudo-twofold symmetry axis of TPT dimer lying between and parallel to the planes of TPT monomers. It follows from the shown model that the fragments of DNA duplexes may make an angle of 60°–80° at the contact site, TPT dimer forms two

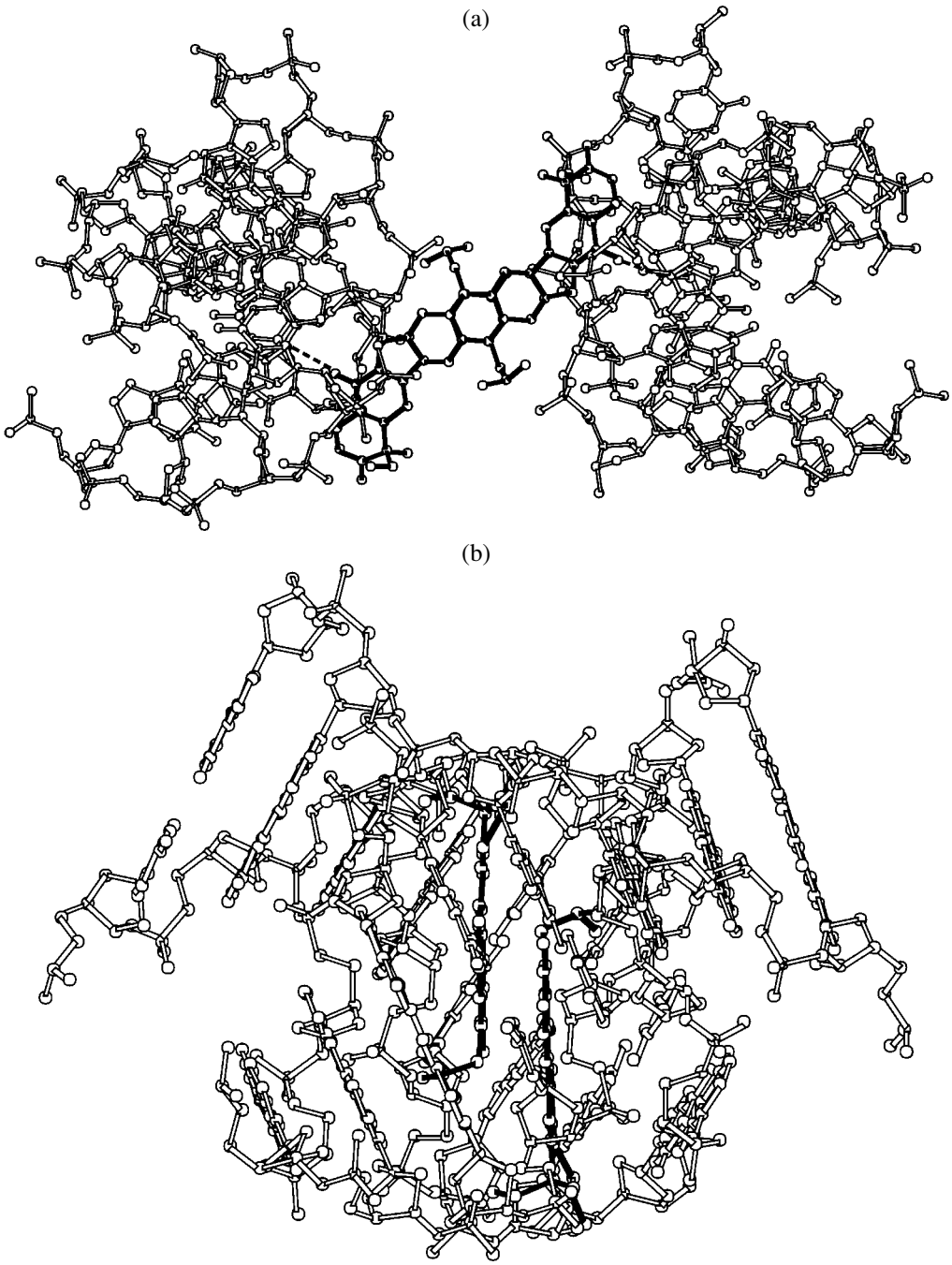

Fig. 8. Molecular model for the complex of TPT dimer (bold) of the **I** type with two crossed sites of duplex of the same DNA. (a) View from the side of helical twofold symmetry axis of TPT dimer perpendicular to its chromophore plane. Dotted lines show hydrogen bonds between keto groups of the rings D of TPT and 2-amino groups of guanines; (b) view from the side of the pseudo-twofold symmetry axis of TPT dimer located between and parallel to the planes of TPT monomers.

hydrogen bonds between its keto groups at the D rings and the 2-amino groups of guanines of neighboring duplexes. In the model of such a complex with TPT dimers of the **III** type, the oxygens of phosphate groups belonging to neighboring duplexes prove to be drawn together to 3.5 Å as in the G4 structure (not shown). We failed to build molecular models of complexes for the TPT dimers of the **II** type because of interpenetration of TPT and DNA atoms.

It is of interest that, in the molecular models of TPT complex with both linear and circular supercoiled DNAs, the chromophore planes of TPT dimers form almost the same angle of ~35° with the plane of bases.

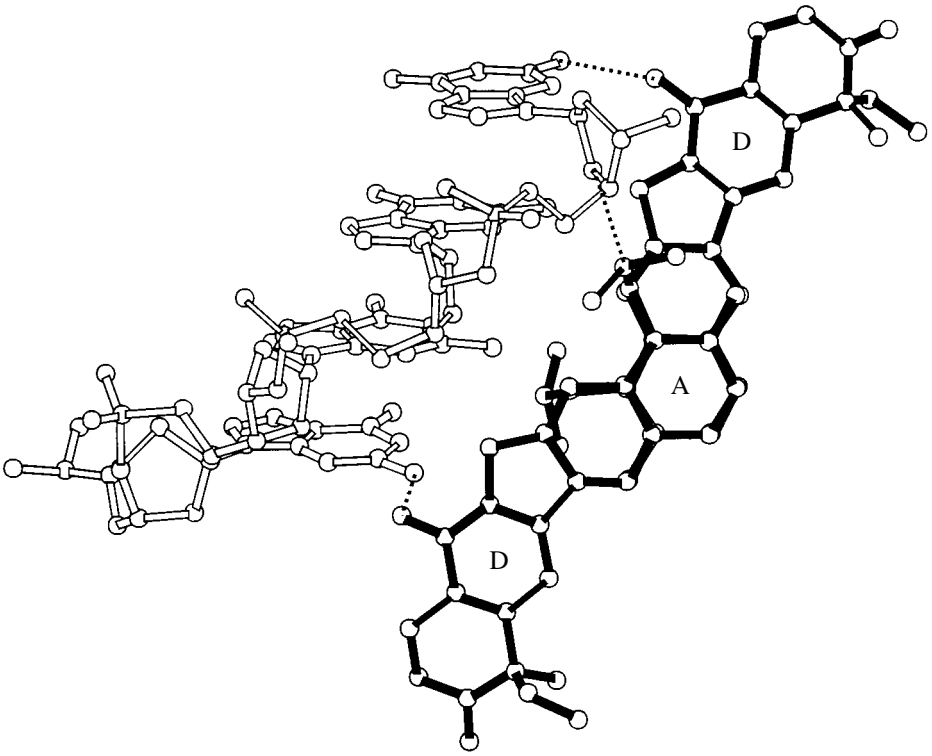

Fig. 9. Molecular model for the complex of TPT dimer (bold) of the **II** type with $(dG)_4$. Dotted lines show hydrogen bonds.

Molecular Model of Interaction of TPT Dimers with Deoxyguanosine

Raman spectroscopy has shown that only the spectrum of TPT–dG complexes is similar to that of TPT–DNA complexes but differs considerably for other nucleosides (dA, dT, dC, and dI) [31]. Consequently, the same atom groups in DNA and dG molecules interact with the same atom groups in TPT molecule. Figure 9 shows a molecular model for the complex of TPT dimer of the **II** type with dG. As in the previous case, the formation of this complex is independent of solution ionic strength. To build the model, we used $(dG)_4$ in geometry similar to the geometry of the B form of DNA. Guanines participate in stacking interaction with each other, while the 2-amino group of the first and the fourth guanine form hydrogen bonds with the keto group of the D rings of TPT dimer. Additional hydrogen bond is possible between the nitrogen atom of dimethylaminomethylene group of TPT and the oxygen atom of deoxyribofuranose ring. We purposefully selected $(dG)_4$ rather than four dG to emphasize that, within the framework of this model, the stacking between dG molecules could be the same as in $(dG)_4$. dG is the sole nucleoside capable of forming stacks in solution. However, this capability is not displayed under our conditions as follows from CD spectrum (see Fig. 10). Indeed, this spectrum shows neither considerable molar dichroism at 250 nm nor additional maximum at 290 nm, which are the features of "stacking" or G4 structure [39]. However, these features are characteristic of only extended stacks of dG tetrads, therefore the CD spectra may indicate the absence of only this type of stacks rather than the absence of any stacking interaction as in the model in Fig. 9. TPT dimers of the **I** and **III** types provide no possibility to build a molecular model of a complex where additional stabilization would arise owing to the stacking interaction between guanines.

TPT is capable of binding not only to double-stranded, but also to single-stranded polymers [16]; it should be taken into account that the suggested model describes the interaction of TPT dimers not only with dG but also with single-stranded oligo(dG).

On the basis of X-ray studies of the topo I–DNA complex, several attempts were made to build hypothetical models of **ternary** complex CPT–topo I–DNA [40–42]. Thus, Redinbo *et al.* [40] suppose CPT to bind to topo I–DNA complex after cleavage of the sugar-phosphate backbone of one DNA strand. As a result, CPT replaces guanine at position (+1) of cleaved DNA strand, which flips out from DNA, while the keto group of the D ring forms a hydrogen bond with the 6-amino group of cytosine at position (+1) of the intact complementary DNA strand.

The model by Fan *et al.* [41] presumes pseudointercalation of CPT between thymine at position (–1) and guanine at position (+1). The keto group of the D

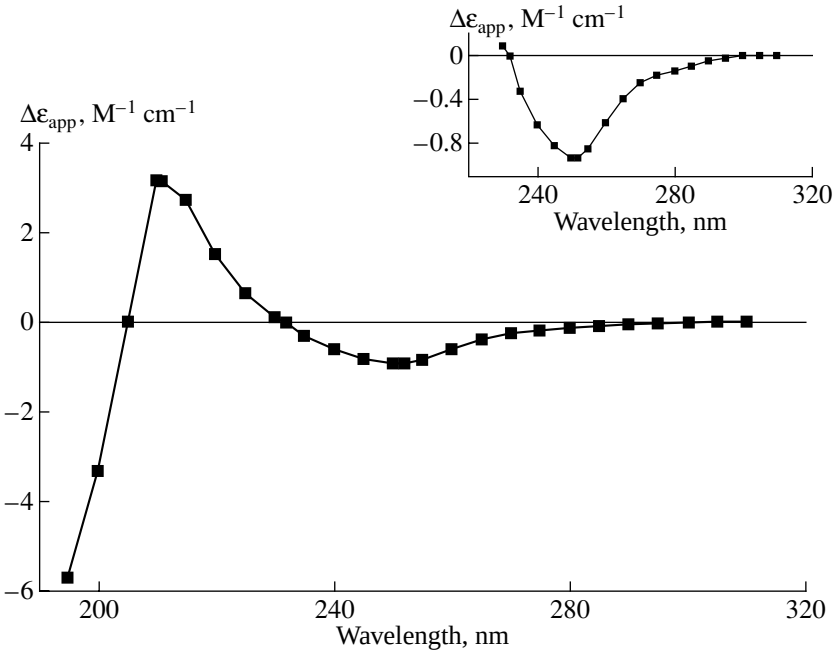

Fig. 10. The spectra of apparent molar circular dichroism $\Delta\varepsilon_{app}$ of dG. Concentration of dG is $3.4 \cdot 10^{-3}$ M. The long-wavelength region of spectrum of $\Delta\varepsilon_{app}$ for dG is shown in the upper right-hand corner. Buffer as in Fig. 3.

ring makes a hydrogen bond with the hydroxy group of the deoxyribose at the 5'-terminus in the cleavage site.

Using Molecular Operating Environment, Kerrigan and Pilch [42] considered models for three CPT orientations including opposite ones. In all orientations, CPT intercalation is suggested between thymine at position (–1) and guanine at position (+1). In the best-energy model, CPT intercalates in such a manner that its long axis is virtually perpendicular to the direction of hydrogen bonds between guanine and cytosine. In so doing, ring E is in the DNA minor groove, while ring A is in the major groove. Formation of the following hydrogen bonds is assumed: (1) in the minor groove, bifurcated hydrogen bond of ring E hydroxy group with N3 of guanine at position (+1) and the deoxyribofuranose oxygen of guanine at position (+2); (2) in the major groove, bifurcated hydrogen bond between the N1 of CPT with the N1 of thymine at position (–1) and the nitrogen of NH_2 of adenine making a Watson–Crick pair with this thymine.

The building of a model of TPT(CPT)–DNA complex without participation of topo I is rather reasonable as the first step in studying the inhibiting function of CPT in the ternary complex, inasmuch as CPT not only inhibits one of the steps of topo I action on DNA, but changes the specificity of DNA cleavage by the enzyme when bound in the ternary complex [7]. Moreover, one gets an impression that it is CPT (TPT) binding to DNA that determines the formation specificity of the overall complex.

We suggest a model that explains from a single viewpoint the complexation of TPT (CPT) dimer with linear, circular supercoiled DNA, and deoxyguanosine in the **absence** of the enzyme. TPT dimer (in the case of binding to DNA) is located in the minor groove. The keto groups of ring D form hydrogen bonds with the 2-amino groups of guanines. Other functional groups of TPT (which distinguish it from CPT), dimethylaminomethylene and hydroxy groups of ring A, do not participate in the interaction with DNA as a rule. The C7 of TPT is 6–8 Å from the N3 of guanine neighboring the one hydrogen-bonded to TPT, which agrees well with the data on the covalent linking of CPT derivative containing a C7-chloromethyl to the N3 atom of purine at position (–1) [15]. The suggested model of interaction of TPT dimers with DNA may be general for all molecules of the CPT family, taking into account that: (1) CPT molecule form dimers like TPT [21]; (2) these dimers have the same elements of symmetry (see above); (3) the projections of long-wavelength ETDMs on the plane of rings A–D are parallel to each other; (4) when CPT molecules bind to DNA in solutions of low ionic strength, they form an angle of 57°–59° with the DNA long axis [36], whereas TPT molecule forms an angle of 62°–64° (determination of the angles was carried out under the same assumptions).

In this work we have shown for the first time that in solutions of **low ionic strength**:

(1) TPT binds preferably to GC base pairs;

(2) TPT binds to DNA in dimeric form better than in monomeric form;

(3) the suggested models of TPT dimers can describe the formation of intermolecular complexes: with DNA duplexes arranged in parallel, with circular supercoiled DNA, and with deoxyguanosine.

Thus, TPT (and perhaps the whole camptothecin family) proved to represent a new class of DNA-specific ligands, which are neither intercalators nor classical minor-groove binders; the main manner of their biological action is the formation of dimeric "bridges" between two DNA duplexes.

ACKNOWLEDGMENTS

This work was partly supported by the Russian Foundation for Basic Research (projects nos. 01-04-48657, 01-03-32669, 00-15-97834, and 00-04-48105).

REFERENCES

1. Strel'tsov, S.A., Mikheikin, A.L., Grokhovsky, S.L., Oleinikov, V.A., and Zhuze, A.L., *Mol. Biol.*, 2002, vol. 36, pp. 511–524.
2. Wall, M.E., Wani, M.C., Cook, C.E., Palmer, K.H., McPhail, A.T., and Sims, G.A., *J. Am. Chem. Soc.*, 1966, vol. 88, pp. 3888–3890.
3. Kingsbury, W.D., Boehm, J.C., Jakas, D.R., Holden, K.G., Hecht, S.M., Gallagher, G., Caranfa, M.J., McCabe, F.L., Faucett, L.F., Johnson, R.K., and Hertzberg, R.P., *J. Med. Chem.*, 1991, vol. 34, pp. 98–107.
4. Chen, A.Y., and Liu, L.F., *Annu. Rev. Pharmacol. Toxicol.*, 1994, vol. 94, pp. 194–218.
5. Hsiang, Y.H., Hertzberg, R.P., Hecht, S., M., and Liu, L.F., *J. Biol. Chem.*, 1985, vol. 260, pp. 14873–14878.
6. Hertzberg, R.P., Busby, R.W., Caranfa, M.J., Holden, K.G., Johnson, R.K., Hecht, S.M., and Kingsbury, W.D., *J. Biol. Chem.*, 1990, vol. 265, pp. 19287–19295.
7. Li, L.H., Frase, T.J., Olin, E.J., and Bhuyan, B.K., *Cancer Res.*, 1972, vol. 32, pp. 2643–2650.
8. Kuwahara, J., Suzuki, T., Funakoshi, K., and Sugiura, J., *Biochemistry*, 1986, vol. 25, pp. 1216–1221.
9. Rothenberg, M.L., *Ann. Oncol.*, 1997, vol. 8, pp. 837–855.
10. Strel'tsov, S.A., Mikheikin, A.L., and Nechipurenko, Yu.D., *Mol. Biol.*, 2001, vol. 35, pp. 442–450.
11. Leteurtre, F., Fesen, M., Kohlhagen, G., Kohn, K.W., and Pommier, Y., *Biochemistry*, 1993, vol. 32, pp. 8955–8962.
12. Yang, D., Strode, T., Spielmann, H.P., Wang, H.-J., and Burke, T.G., *J. Am. Chem. Soc.*, 1998, vol. 120, pp. 2979–2980.
13. Chourpa, I., Riou, J.-F., Millot, J.-M., Pommier, Y., and Manfait, M., *Biochemistry*, 1998, vol. 37, pp. 7284–7291.
14. Jaxel, C., Capranico, J., Karrigan, D., Kohn, K.W., and Pommier, Y., *J. Biol. Chem.*, 1991, vol. 266, pp. 20418–20423.
15. Pommier, Y., Kolhlagen, G., Kohn, K.W., Leteurte, F., Wani, M.C., and Wall, M.E., *Proc. Natl. Acad. Sci. USA*, 1995, vol. 92, pp. 8861–8865.
16. Yao, S., Murali, D., Seetharamulu, P., Haridas, K., Petluru, P.N.V., Reddy, D.G., and Hausheer, F.H., *Cancer Res.*, 1998, vol. 58, pp. 3782–3786.
17. Fukada, M., *Biochem. Pharmacol.*, 1985, vol. 34, pp. 1225–1230.
18. Strel'tsov, S.A., Grokhovsky, S.L., Kudelina, I.A., Oleinikov, V.A., and Zhuze, A.L., *Mol. Biol.*, 2001, vol. 35, pp. 432–441.
19. Wells, R.D., Larson, J.E., Grant, R.C., Shortle, B.E., and Cantor, C.R., *J. Mol. Biol.*, 1970, vol. 54, pp. 465–497.
20. Makarov, V.L., Strel'tsov, S.A., Vengerov, Yu.Yu., Khorlin, A.A., and Gurskii, G.V., *Mol. Biol.*, 1983, vol. 17, pp. 1089–1101.
21. McPhail, A.T. and Sim, G.A., *J. Chem. Soc. (B)*, 1968, pp. 923–928.
22. Nabiev, I., Choupra, I., and Manfait, M., *J. Phys. Chem., B*, 1994, vol. 98, pp. 1344–1350.
23. Oleinikov, V., Mochalov, K., Ustinova, O., Zhuze, A., Streltsov, S., Sukhanova, A., Jardillier, J.C., and Nabiev, I., *Anticancer Res.*, 2001, vol. 21, pp. 1552–1553.
24. Mochalov, K.E., Ustinova, O.A., Strel'tsov, S.A., Grokhovsky, S.L., Zhuze, A.L., Nabiev, I.R., Sukhanova, A.V., and Oleinikov, V.A., *Opt. Spektrosk.*, 2002, vol. 93, pp. 537–545.
25. Rodger, A. and Norden, B., *Circular Dichroism and Linear Dichroism*, Oxford University Press: 1997, p. 150.
26. Lyng, R., Rodger, A., and Norden, B., *Biopolymers*, 1991, vol. 31, pp. 1709–1720.
27. Nabiev, I., Fleury, F., Kudelina, I., Pommier, Y., Charton, F., Riou, J.-F., Alix, A.J.P., and Manfait, M., *Biochem. Pharmacol.*, 1998, vol. 55, pp. 1163–1174.
28. Strel'tsov, S.A. and Nechipurenko, Yu.D., *Bioorg. Khim.*, 1999, vol. 25, pp. 584–590.
29. Mochalov, K.E., Strel'tsov, S.A., Ermishov, M.A., Grokhovsky, S.L., Ustinova, O.A., Sukhanova, A.V., Zhuze, A.L., Nabiev, I.R., and Oleinikov, V.A., *Opt. Spektrosk.*, 2002, vol. 93, pp. 454–462.
30. Norden, B., *Appl. Spectr. Rev.*, 1978, vol. 14, pp. 157–284.
31. Streltsov, S., Sukhanova, A., Mikheikin, A., Grokhovsky, S., Zhuze, A., Kudelina, I., Mochalov, K., Oleinikov, V., Jardillier, J.-C., and Nabiev, I., *J. Phys. Chem. B*, 2001, vol. 105, pp. 9643–9652.

32. Wang, X., Zhou, X., and Hecht, S.M., *Biochemistry*, 1999, vol. 38, 4374–4381.

33. Streltsov, S.A., Semenov, T.E., and Moroz, O.V., *J. Biomol. Struct. Dynam.*, 1993, vol. 10, pp. 763–784.

34. Streltsov, S.A., Borodina, M.V., and Semenov, T.E., *J. Biomol. Struct. Dynam.*, 1996, vol. 14, pp. 357–363.

35. Nechipurenko, Yu.D., Strel'tsov, S.A., and Evdokimov, Yu.M., *Biofizika*, 2001, vol. 46, pp. 428–435.

36. Bailly, C., Riou, J.-F., Colson, P., Houssier, C., Rodrigues-Pereira, E., and Prudhomme, M., *Biochemistry*, 1997, vol. 36, pp. 3917–3929.

37. Phillips, K., Dauter, Z., Murchi, A.I., Liley, D.M., and Luisi, B., *J. Mol. Biol.*, 1997, vol. 17, pp. 171–182.

38. Zechiedrich, E.L. and Osheroff, N., *EMBO J.*, 1990, vol. 9, pp. 4555–4562.

39. Guschelbauer, W., Chantot, J.-F., and Thide, D., *J. Biomol. Struct. Dynam.*, 1990, vol. 8, pp. 491–511.

40. Redinbo, M.R., Stewart, L., Kuhn, P., Champoux, J.J., and Hol, W.G.J., *Science*, 1998, vol. 279, pp. 1504–1513.

41. Fan, Y., Weinstein, J.N., Kohn, K.W., Shi, L.M., and Pommier, Y., *J. Med. Chem.*, 1998, vol. 41, pp. 2216–2226.

42. Kerrigan, J.E. and Pilch, D.S., *Biochemistry*, 2001, vol. 40, pp. 9792–9798.